

Angular dependence of resistivity in the superconducting state of $\text{Nb}_2\text{Pd}_{0.73}\text{S}_{5.7}$ single crystals

Anil K. Yadav,^{*} Himanshu Sharma, Santosh Kumar, Ujjawal Nandi, and C. V. Tomy[†]

Department of physics, Indian Institute of Technology Bombay, Powai Mumbai 400076 India

Ajay D. Thakur

*School of Basic Sciences, Department of Physics,
Indian Institute of Technology Patna, Patna 800013 India*

Abstract

We report the superconducting anisotropy in $\text{Nb}_2\text{Pd}_{0.73}\text{S}_{5.7}$ single crystals via the magneto-transport and the angular dependent resistivity measurements. The anisotropy parameter Γ is calculated using the scaling approach within the framework of the Ginzburg-Landau theory. The estimated value of Γ close to T_c is found to be ~ 2.4 which decreases with decreasing temperature, indicating the presence of multi-band Fermi surface in this superconductor.

^{*}Electronic address: anilsaciitb@gmail.com

[†]Electronic address: tomy@phy.iitb.ac.in

I. INTRODUCTION

Superconductivity with a $T_c \sim 6.5$ K emerges in the non-superconducting ternary chalcogenide $\text{Nb}_2\text{Pd}_{0.81}\text{Se}_5$ when Se is replaced with S [1]. This superconductor has generated quite an interest among the research community due to its extremely large upper critical fields amongst the known Nb based superconductors as well as due to the possibility of growing long flexible single crystal fibers, both of which are useful for practical applications [1, 2]. In addition to these, there are clear indications that this compound can be classified into a multi-band superconductor with unconventional superconductivity. Structurally, this compound crystallizes in the monoclinic structure with $C2/m$ space group [1–3]. The structure comprises laminar sheets, stacked along the b -axis, consisting of Pb, Nb and S atoms. Each sheet contains two unique building blocks, NbS_6 and NbS_7 , which are inter-linked by the Pd atoms [1, 3, 4]. Yu *et al.* have studied the superconducting phase diagram of $\text{Nb}_2\text{Pd}_{1-x}\text{S}_{5\pm\delta}$ ($0.6 < x < 1$) single crystal fibers by varying all the possible combinations of Pd and S and found that the maximum $T_c \sim 7.43$ K can be achieved with a stoichiometry of $\text{Nb}_2\text{Pd}_{1.1}\text{S}_6$ [2].

One of the important parameters which needs to be determined for this compound is the precise anisotropic parameter (Γ) and its temperature variation [1]. In the conventional approach, the zero temperature upper critical field $H_{c2}(0)$ is determined for the two field directions w.r.t. the crystallographic axes, $H \parallel ab$ and $H \parallel c$, by using the electrical transport or magnetization data near T_c . The anisotropy is then calculated from the ratio of the two direction dependent upper critical fields [5]. Zhang *et al.* [1] have determined the temperature variation of the anisotropy parameter in this compound using the above conventional method by taking the ratio of H_{c2} at each temperature. The extraction method of $H_{c2}(0)$ or H_{c2} is subject to different criteria and formalism which can introduce some uncertainty in the anisotropy (Γ) calculation [6]. Following an approach based on the Ginzburg Landau theory, Blatter *et al.* have suggested a simple alternate way to estimate the anisotropy of a superconductor, known as the scaling approach [7]. In this approach, only one parameter needs to be adjusted which comes out to be the anisotropy parameter, Γ . This in turn limits the uncertainty in the determination of Γ as compared to the conventional approach. Employing the scaling approach, Wen *et al.* have estimated the anisotropy of several Fe-based superconductors such as $\text{NdFeAsO}_{0.82}\text{F}_{0.18}$ [8], $\text{Ba}_{1-x}\text{K}_x\text{Fe}_2\text{As}_2$ [6] and $\text{Rb}_{0.8}\text{Fe}_2\text{Se}_2$ [9]. Shahbazi

et al. have also performed similar studies on $\text{Fe}_{1.04}\text{Se}_{0.6}\text{Te}_{0.4}$ [10] and $\text{BaFe}_{1.9}\text{Co}_{0.1}\text{As}_2$ [11] single crystals and found the anisotropy to be temperature dependent. Here we report the anisotropy estimation of $\text{Nb}_2\text{Pd}_{0.73}\text{S}_{5.7}$ single crystals from the angular dependent resistivity measurements by applying the scaling approach method at different temperatures.

II. METHOD

Single crystal fibers of $\text{Nb}_2\text{Pd}_{0.73}\text{S}_{5.7}$ were synthesized via slow cooling of the charge in the solid state reaction method, as reported in reference [1]. In this synthesis process, the starting raw materials (powder) Nb (99.99%), Pd (99.99%) and S (99.999%) were taken in the stoichiometric ratio of 2:1:6 and mixed in an Ar atmosphere inside a glove box. The well-homogenized mixture was sealed in a long evacuated quartz tube and heated to 800°C at a rate of $10^\circ\text{C}/\text{h}$. After the reaction for 24 hours at this temperature, the reactants were cooled down at a rate of $2^\circ\text{C}/\text{h}$ to 360°C , followed by cooling to room temperature by switching the furnace off. The as-grown sample looked like a mesh of small wires when viewed under an optical microscope. Some part of the as-grown sample was dipped in dilute HNO_3 to remove the bulk material and to pick up a few fiber rods for further measurements. X-ray diffraction (XRD) was performed on powdered $\text{Nb}_2\text{Pd}_{0.73}\text{S}_{5.7}$ single crystal fibres for structure determination. Magnetization measurement was performed using a superconducting quantum interference device - vibrating sample magnetometer (SQUID-VSM, Quantum Design Inc. USA). Angular dependent resistivity was carried out using the resistivity and horizontal rotator options in a physical property measurement system (PPMS) of Quantum Design Inc. USA. Electrical connections were made in four probe configuration using gold wires bonded to the sample with silver epoxy.

III. RESULTS

Figure 1(a) shows the scanning electron microscope (SEM) image of $\text{Nb}_2\text{Pd}_{0.73}\text{S}_{5.7}$ single crystals fibers. It is clear from the image that the fibers grow in different shapes and lengths. Figure 1(b) shows the XRD patterns of powdered $\text{Nb}_2\text{Pd}_{0.73}\text{S}_{5.7}$ single crystals. Rietveld refinement was performed on the powder XRD data using $C2/m$ monoclinic crystal structure of $\text{Nb}_2\text{Pd}_{0.81}\text{Se}_5$ as reference using the FullProf suite software. The lattice parameters ($a =$

12.154(1), $b = 3.283(7)$ and $c = 15.09(9)$) obtained from the refinement were found to be close to the values reported earlier [1, 3], even though the intensities could not be matched perfectly. The (200) peak is found to be the one with the highest intensity even when the XRD was obtained with a bunch of fibers, indicating a preferred orientation of the crystallites along the $(l, 0, 0)$ direction in our powdered samples. Similar preferred orientation was also reported for single crystals in reference [2]. This may be the reason for the discrepancy in the intensities between the observed and the fitted XRD peaks. To confirm the single crystalline nature of the fibers, we have taken the selective area electron diffraction (SAED) pattern of the fibers; a typical pattern is shown in Figure 1(c). The nicely ordered spotted diffraction pattern confirms the single crystal nature of the fibers. Figure 1(d) shows the optical image of a typical cylindrical fiber of diameter $\sim 1.2 \mu\text{m}$ and of length $\sim 1814 \mu\text{m}$, which was used for the four probe electrical resistivity measurements (Figure 1(e) shows the gold wires and silver paste used for the electrical connections).

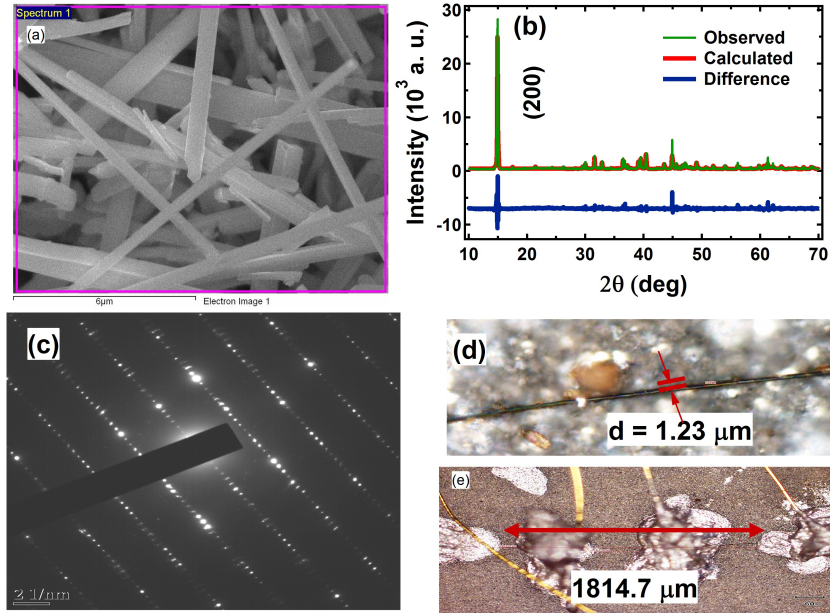


Figure 1: (Color online) (a) SEM image for a bunch of single crystal fibers of $\text{Nb}_2\text{Pd}_{0.73}\text{S}_{5.7}$ single crystals. (b) X-ray diffraction patterns: observed (green), calculated (red) and difference (blue) (c) SAED pattern from a single fiber (d) optical image of a typical cylindrical wire used for transport study (e) Four probe connections on the fiber.

In order to confirm the occurrence of superconductivity in the prepared single crystal samples, magnetization was measured using a bunch of fibers (we could not obtain a single

fiber which gave large enough signal in magnetization). Figure 2 shows a part of the temperature dependent zero field-cooled (ZFC) and field-cooled (FC) magnetization measurements at $H = 20$ Oe. The onset superconducting transition temperature ($T_c^{\text{on};M}$) is observed to be

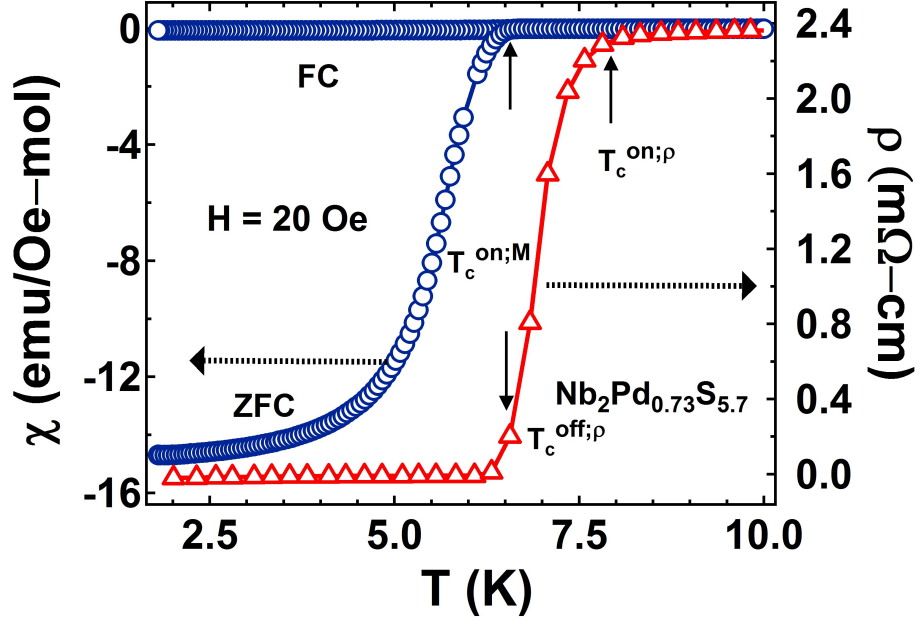


Figure 2: (Color online) Zero field-cooled (ZFC) and field-cooled (FC) magnetization curves at 20 Oe (open circle) and resistivity measurement at zero field (open triangle). Onset superconducting transition temperature, $T_c^{\text{on};M}$, from magnetization and offset superconducting transition temperature, $T_c^{\text{off};\rho}$, from resistivity measurement confirm the T_c of $\text{Nb}_2\text{Pd}_{0.73}\text{S}_{5.7}$ superconductor.

~ 6.5 K which is taken to be the bifurcation point between the ZFC and the FC curves. In order to confirm the superconducting nature of the grown single crystal fibers, resistivity was measured using one of the fibers removed from the ingot. We have plotted a part of this resistivity measurement (in zero applied magnetic field) in Fig. 2 along with the magnetization curve. The transition temperature $T_c^{\text{off};\rho}$, which is defined as the temperature at which resistivity drops to 10% of the normal state resistivity at 8 K, matches well with the onset temperature from the magnetization, $T_c^{\text{on};M}$ as well as the T_c reported in reference [1, 2]. However, the onset transition temperature from resistivity ($T_c^{\text{on};\rho}$: the temperature at which resistivity drop to 90%) is found to be ~ 7.8 K, which is comparable to the optimized maximum T_c for this compound reported by Yu *et al.* [2]. The narrow superconducting transition width ($\Delta T_c \sim 1.3$ K) in resistivity indicates the quality of the single crystal fibers.

The residual resistivity ratio ($RRR \approx \frac{R(300\text{K})}{R(8\text{K})}$), which indicates the metallicity of a material, is found to be 3.4 for our sample. This value of RRR is much less than the corresponding value for good conductors, which indicates that this compound belongs to the class of bad metals.

In order to obtain an estimate of the upper critical field for this fibers, resistivity was measured in different applied magnetic fields upto 90 kOe which are shown in Figs. 3(a) and 3(c). Since we cannot assign a growth direction for the cylindrical single crystal fibers, we

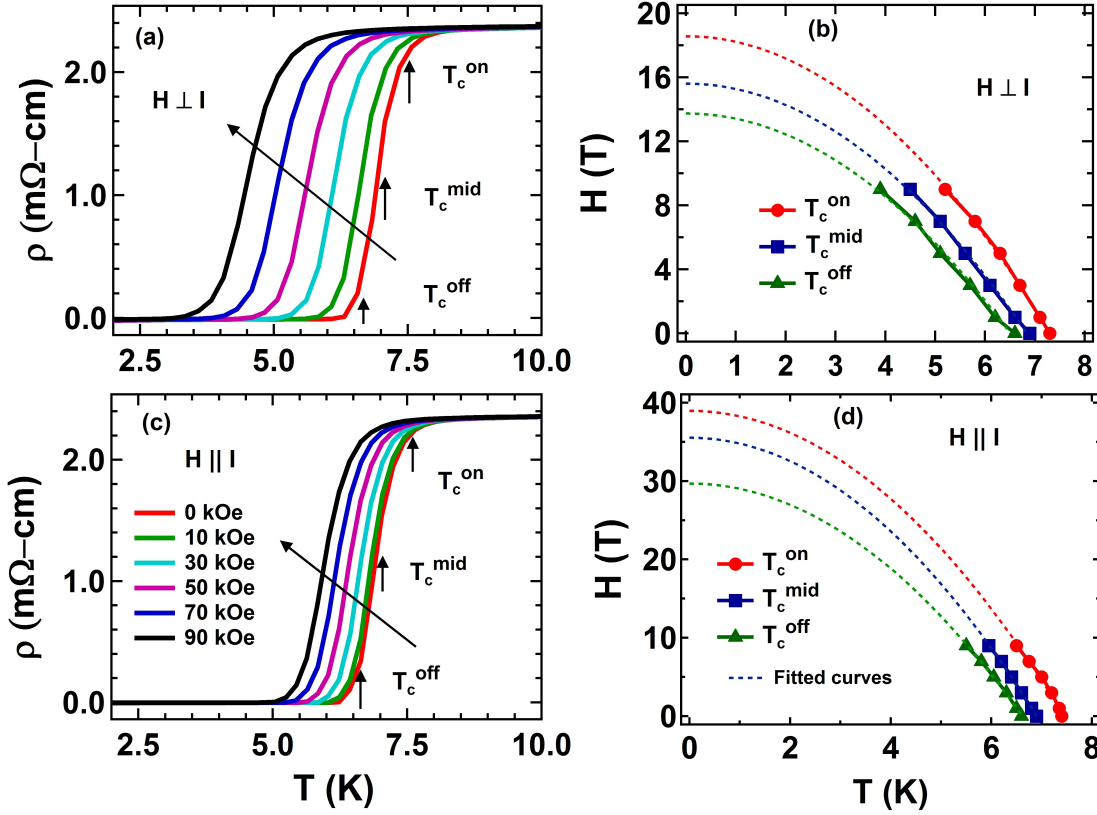


Figure 3: (Color online) Temperature dependent resistivity plots at applied fields from 0 kOe to 90 kOe (a) for $H \perp l$ (d) for $H \parallel l$ directions. (b) and (d) corresponding H - T phase diagrams at T_c^{on} (90% ρ_n), T_c^{mid} (50% ρ_n) and T_c^{off} (10% ρ_n), where ρ_n is the normal state resistivity at 8 K. Dashed curves are fitting curves using the empirical formula, $H_{c2}(0) = H_{c2}(T)(1 - (T/T_c)^2)$ and extrapolated up to zero temperature to extract the $H_{c2}(0)$.

assign the measurements as $H \parallel l$ (along the length of the fiber; current direction) and $H \perp l$ (field perpendicular to the length/current), respectively. The three transition temperatures, T_c^{on} , T_c^{mid} and T_c^{off} are marked in the figure using the criteria, 90% ρ_n , 50% ρ_n and 10% ρ_n

(ρ_n is taken as the resistivity at 8 K), respectively. The T_c is found to decrease at a rate of 0.05 K/kOe and 0.02 K/kOe for $H \perp l$ and $H \parallel l$ directions, respectively. These three transition temperatures are plotted in an H - T phase diagram in Figs. 3(b) and 3(d) for both the directions. These H - T curves were fitted using the empirical formula, $H_{c2}(0) = H_{c2}(T)(1 - (T/T_c)^2)$ [2], and extrapolated to the zero temperature to extract the $H_{c2}(0)$ values. The $H_{c2}(0)$ values are estimated to be 180 kOe and 390 kOe at T_c^{on} for $H \perp l$ and $H \parallel l$, respectively. The anisotropy parameter Γ , taken as the ratio between the two $H_{c2}(0)$ values is found to be ~ 2.2 .

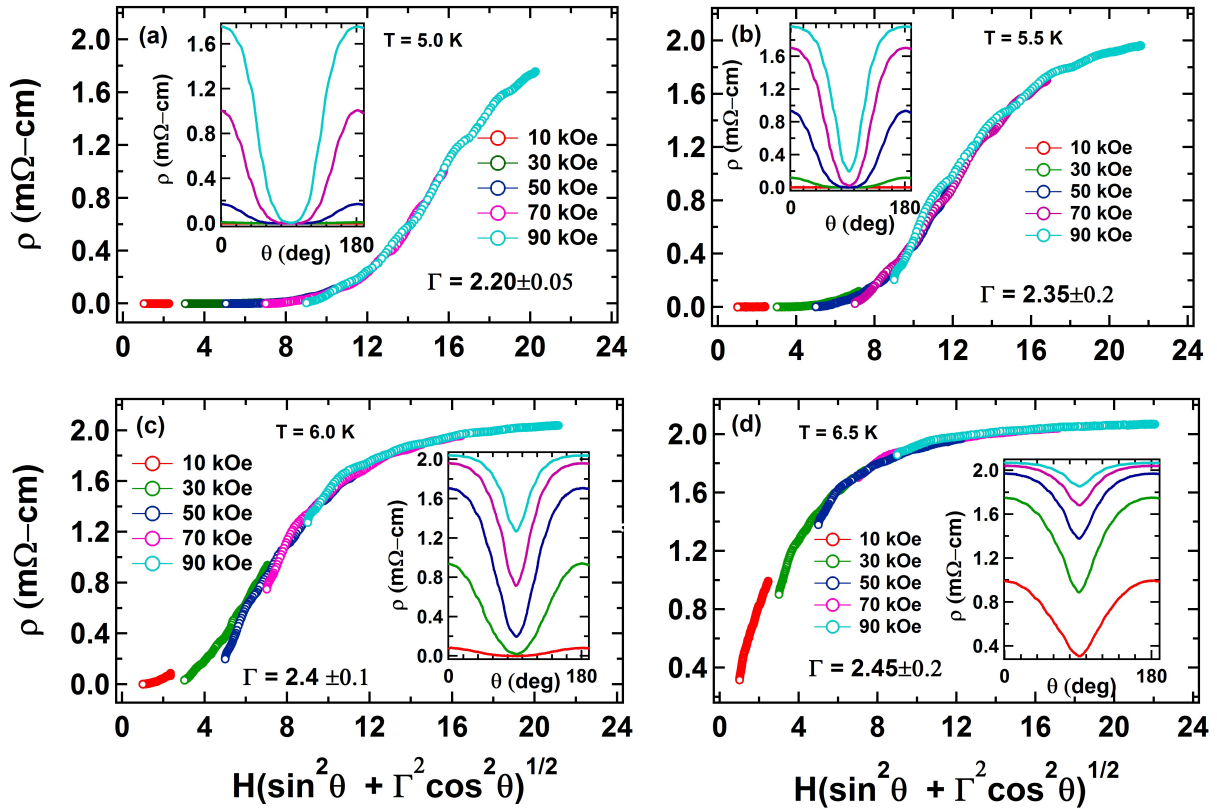


Figure 4: (Color online) The main panels (a) to (d) show resistivity (ρ) plots as a function of scaling field $\tilde{H} = H \sqrt{\sin^2\theta + \Gamma^2 \cos^2\theta}$ at fields 10 kOe, 30 kOe, 50 kOe, 70 kOe and 90 kOe at temperatures (a) 5 K (b) 5.5 K (c) 6.0 K (d) 6.5 K. The inset panels (a) to (d) show the ρ vs θ (angle between the current direction and the magnetic field).

In order to corroborate the Γ values further, we have measured the angular dependent resistivity ($\rho(\theta)$) at different magnetic fields at certain temperatures close to T_c . The insets of Figs. 4(a), (b), (c) and (d) show $\rho(\theta)$ curves at 10 kOe, 30 kOe, 50 kOe, 70 kOe and 90 kOe

for $T = 5.0$ K, 5.5 K, 6.0 K and 6.5 K, respectively. All the $\rho(\theta)$ curves show a symmetric dip at $\theta = 90^\circ$ and a maximum at 0° and 180° . In all the curves, the center of the dip shifts from zero to non-zero resistivity as the temperature and the field increases. The main panel of the Fig. 4 shows rescaled $\rho(\theta)$ curves of 10 kOe, 30 kOe, 50 kOe, 70 kOe and 90 kOe fields at temperatures (a) 5.0 K (b) 5.5 K (c) 6.0 K and (d) 6.5 K, respectively using the rescaling function,

$$\tilde{H} = H \sqrt{\sin^2\theta + \Gamma^2\cos^2\theta} \quad (1)$$

All the rescaled curves for a given temperature are now isotropic, i.e., they fall on the same curve. The single parameter Γ , which was adjusted for making the anisotropic resistivity curves collapse into a single curve, gives the anisotropy at that temperature. Figure 5 shows the dependence of anisotropy ($\Gamma(T)$) with temperature obtained from the angular resistivity data. There is a slight increase in anisotropy as the temperature approaches T_c .

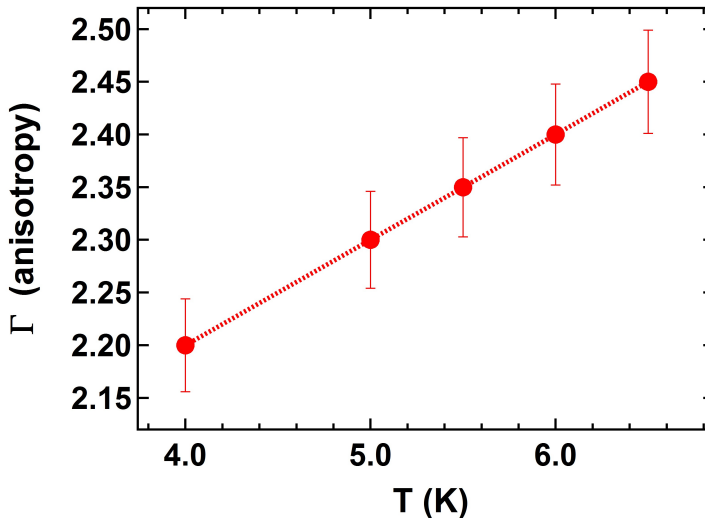


Figure 5: (Color online) Anisotropy variation with temperature measured from angular dependent resistivity.

Similar behaviour is also seen in other Fe-based superconductors such as $\text{Ba}_{0.6}\text{K}_{0.4}\text{Fe}_2\text{As}_2$, $\text{Ba}(\text{Fe}_{0.92}\text{Co}_{0.08})_2\text{As}_2$ and $\text{Rb}_{0.8}\text{Fe}_2\text{Se}_2$ [9–11]. This kind of temperature dependent $\Gamma(T)$ is generally taken as reminiscent of multi-band anisotropic superconductors [12–15]. The density functional theory (DFT) calculations indeed has shown that the $\text{Nb}_2\text{Pd}_{0.81}\text{S}_5$ superconductor is a multi-band superconductor [1]. Compared to MgB_2 [16, 17] and cuprate superconductors [18] the anisotropy of $\text{Nb}_2\text{Pd}_{0.73}\text{S}_{5.7}$ [8] is very small; however, it is compa-

rable with some of the Fe-based Fe-122 superconductors [19].

In conclusion, we have successfully synthesized the $\text{Nb}_2\text{Pd}_{0.73}\text{S}_{5.7}$ single crystal fibers via slow cooling solid state reaction method. The magnetic field dependence of resistivity as a function of the angle between the applied field and the current direction is measured at different temperatures. The angular dependent resistivity $\rho(\theta, H)$ data measured at different fields for a certain temperature, have been properly scaled using a scaling function within the anisotropic Ginzburg Landau theory. The anisotropy $\Gamma(T)$ is found to be ~ 2.5 near T_c and decreases slowly with decreasing temperature, which is attributed to the multi-band nature of the superconductor.

Acknowledgments

Authors acknowledge the use of IITB central facilities. One of the authors (AKY) wants to acknowledge to Council of Scientific and Industrial Research (CSIR) for financial support during PhD.

-
- [1] Q. Zhang, G. Li, D. Rhodes, A. Kiswandhi, T. Besara, B. Zeng, J. Sun, T. Siegrist, M. D. Johannes, L. Balicas, *Scientific Reports*, **3**, 1446 (2013). H. Yu, M. Zuo, L. Zhang, S. Tan, C. Zhang, Y. Zhang, *J. Am. Chem. Soc.* **135**, 12987 (2013).
 - [2] H. Yu, M. Zuo, L. Zhang, S. Tan, C. Zhang, Y. Zhang, *J. Am. Chem. Soc.* **135**, 12987 (2013).
 - [3] R. Jha, B. Tiwari, P. Rani, V. P. S. Awana, arXiv:1312.0425 (2013).
 - [4] D. A. Keszler, J. A. Ibers, M. Y. Shang and J. X. Lu, *J. solid state chem.* **57**, 68 (1985).
 - [5] W. E. Lawrence and S. Doniach, in *Proceedings of the 12th International Conference Low Temperature Physics*, edited by E. Kanda Keigaku, Tokyo (1971).
 - [6] Z. S. Wang, H. Q. Luo, C. Ren, H. H. Wen, *Phys. Rev. B* **78**, 140501(R) (2008).
 - [7] G. Blatter, V. B. Geshkenbein, and A. I. Larkin, *Phys. Rev. Lett.* **68**, 875 (1992).
 - [8] Y. Jia, P. Cheng, L. Fang, H. Yang, C. Ren, L. Shan, C. Z. Gu, H. H. Wen, *Sup. Science and Technology* **21**, 105018 (2008).
 - [9] C. H. Li, B. Shen, F. Han, X. Zhu, and H. H. Wen, *Phys. Rev. B* **83**, 184521 (2011).

- [10] M. Shahbazi, X. L. Wang, S. X. Dou, H. Fang, and C. T. Lin, *J. Appl. Phys.* **113**, 17E115 (2013).
- [11] M. Shahbazi, X. L. Wang, S. R. Ghorbani, S. X. Dou, and K. Y. Choi, *Appl. Phys. Lett.* **100**, 102601 (2012).
- [12] Q. Han, Y. Chen and Z. D. Wang, *EPL* **82**, 37007 (2008).
- [13] K. Sasmal, B. Lv, Z. Tang, F. Y. Wei, Y. Y. Xue, A. M. Guloy, and C. W. Chu , *Phys. Rev. B* **81**, 144512 (2010).
- [14] C. Ren, Z. S. Wang, H. Q. Luo, H. Yang, L. Shan, and H. H. Wen, *Phys. Rev. Lett.* **101**, 257006 (2008).
- [15] V. Cvetkovic, Z. Tesanovic, *Europhysics Letters* **85**, 37002 (2009).
- [16] A. Rydh, U. Welp, A. E. Koshelev, W. K. Kwok, G. W. Crabtree, R. Brusetti, L. Lyard, T. Klein, C. Marcenat, B. Kang, K. H. Kim, K. H. P. Kim, H.-S. Lee, and S.-I. Lee , *Phys. Rev. B* **70**, 132503 (2004).
- [17] K. Takahashi, T. Atsumi, N. Yamamoto, M. Xu, H. Kitazawa, and T. Ishida, *Phys. Rev. B* **66**, 012501 (2002).
- [18] C. P. Poole, Jr. H. A. Farach, J. Richard. Creswick, *Superconductivity* (Elsevier) (2007).
- [19] M. Rotter, M. Tegel, and D. Johrendt, *Phys. Rev. Lett.* **101**, 107006 (2008).